Islamic Azad University

Journal of

Optoelectronical Nanostructures

Autumn 2017 / Vol. 2, No. 4

First–Principle Calculation of the Electronic and Optical Properties of Nanolayered ZnO Polymorphs by PBE and mBJ Density Functionals

Seyed Javad Mousavi[*, 1]

[1] Department of Physics, Rasht Branch, Islamic Azad University, Rasht, Iran

(Received 8 Sep. 2017; Revised 16 Oct. 2017; Accepted 21 Nov. 2017; Published 15 Dec. 2017)

Abstract: First principle calculations of nanolayered ZnO polymorphs (Wurzite–, Zinc blende–, Rocksalt–structures) in the scheme of density functional theory were performed with the help of full potential linear augmented plane wave (FP-LAPW) method. The exchange - correlation potential is described by generalized gradient approximation as proposed by Perdew–Burke–Ernzrhof (GGA–PBE) and modified Becke–Johnson (mBJ) approximation. The electronic behavior and the optical properties of the structures are investigated and compared to experimental data, where available. The electronic structure of w–ZnO and z–ZnO revealed a 3.01 eV and 2.59 eV direct energy gap in (Γ→Γ) direction by applying mBJ potential. In contrast to w– and z–ZnO the electronic structure of r–ZnO shows an indirect 2.81 eV energy gap in (Γ→L) direction. Reflectivity, transmittance and refractive index spectra for three nano layered of ZnO phases in Uv – visible region have been calculated. The electron effective mass values at the bottom of conduction band were evaluated for the three geometries.

Key words: ZnO polymorphs, DFT, band structure, effective mass, optical properties.

1. INTRODUCTION

ZnO has caught considerable interest in the past 20 years due to its technological importance in various fields, especially as transparent conducting oxide (TCO) [1]. In the recent years, ZnO based materials including p–type semiconductors, magnetic semiconductors, quantum wells, heterostructures, and nanostructures were widely studied [2].

Experimentally ZnO occurs in three structures: Wurtzite (B4), Zinc blende (B3) and Rocksalt (B1) [3]. ZnO with the structures of the Zinc blende (Z–ZnO) and Rocksalt (R–ZnO) are the two metastable phases that have been well studied. The

* Corresponding author. E-mail: **yabed203@gmail.com**

B4 phase transits to the B1 phase at ~10GPa [4]. Bulk ZnO is known to crystallize only in the hexagonal Wurtzite (W–ZnO) structure under normal conditions.

Experimental work involving ZnO has progressed tremendously over the years; however reporting of theoretical work related to the compilation of ZnO polymorphs is scarce. Nevertheless, theoretical calculations of the pertinent electronic and optical properties are very rare. Nearly all theoretical works have been concentrated on the pressure–induced effects on phase transitions [5–7]. Using CASTEP package, X. Si *et al.* investigated the band structure, density of states (DOS) and optical properties of Mg doped and Mg–Al co–doped W–ZnO by adopting the first–principles calculation of plane wave ultra–soft pseudo–potential technology based on the density functional theory (DFT) [8]. A.A. Peyghan and M. Noei have studied the alkali and alkaline earth metal doped ZnO nanotubes using unrestricted B3LYP functional with LANL2DZ basis sets [9]. Berrezoug *et al.* used generalized gradient approximation and effective Engel–Vosko (GGA–EV) to calculate the structural, electronic, and optical properties of W– and Z–ZnO phases and compared the results with those obtained by GGA–PBE [10]. However, the results particularly on the bandgap value were far from the experimental values. J. Wrobel and J. Piechota calculated the electronic properties of ZnO polymorphs within the LDA+U approximation [3]. By varying the Coulomb interaction U–parameter in VASP package, they managed to get E_g=2.82 eV, 2.20 eV, and 2.94 eV for W–, Z–, and R–ZnO, respectively. These results are better than that reported by Berrezoug *et al.* though still are very different from the experimental values. Using the Vienna ab initio simulation package (VASP) based on DFT, Kuang et al. studied the pressure induced effects on solid–solid phase transition, electronic band structures and elasticity of zinc oxide polymorphs [5]. They employed the so–called PBEsol [11] functional as a revised GGA–PBE. They observed that the fundamental gap increased with increasing pressure. They achieved better agreement between the evaluated and experimental values than the calculated bandgaps through other methods. The effective masses of the structures at meaningful pressures were also estimated.

Most of the previous studies present underestimated/overestimated bandgap values besides giving contradictory nature of bandgap nature as well. The LDA as well as GGA approaches to DFT often fail to describe systems with localized (strongly correlated) d and f electrons. In order to obtain a correct bandgap, many theoretical studies have been done recently. Altogether, the DFT+Ud shows a low improvement of the band gap and only applied to the d orbital of transition metals with the necessity to know the adjustable Hubbard parameter [12]. Recently, the modified version of semi–local Becke–Johnson (mBJ) [13] exchange–correlation potential that proposed by Tran and Blaha [14], can achieve a relevant correction with a low cost of calculations.

On the other hand, a comprehensive first principles DFT–FLAPW study for different phases of nanolayered ZnO is rarely found in the literature. Moreover,

mostly work is at the level of standard LDA/GGA, which is known for their underestimation of bandgap results. Therefore, it is very important to perform study to insight view regarding optoelectronic properties particularly optical properties. In this study, we use GGA–PBE and GGA–mBJ in order to study the structural, electronic, and optical properties of nanolayered ZnO polymorphs. Moreover, for the sake of completeness, the effective masses will be calculated.

2. THEORETICAL MODEL AND COMPUTATIONAL METHOD

Computational methods presented in this study are based on DFT first–principle approach implemented within the Wien2k software package [15]. The calculations of electronic and optical properties were adopted for GGA–PBE and GGA–mBJ functional. Experimentally obtained crystal data for lattice parameters was used as a starting point to simulate the structure of ZnO. The radius of muffin–tin (RMT) sphere values for Zn and O atoms were taken to be 1.01 and 0.86 Å, respectively. The plane wave cut off parameters were RMT * K_{max}= 8.0 $(Ryd)^{1/2}$. In this study, we consider a 2 × 2 × 2 supercell of a W–, Z–, and R–ZnO, which contains 32 atoms (16 Zn atoms and 16 O atoms). In calculations, the Brillouin zone integrations were performed using 14×14×14 K–points mesh sampling for Z– and R–ZnO and 13×13×9 for hexagonal polymorphs. The chosen plane wave cutoff and the number of K–points allowed a convergence of the total energy to within 10^{-5} Ryd/unit cell.
A ZnO (001) slab surface model is constructed using the supercell approach and periodic boundary conditions. In order to use the plane-wave basis set which is periodic in nature, the corresponding slab is repeated in the third direction with the slabs separated by 2 thick enough vacuum regions (10 Å upper and bottom of the slab). The thickness of a slab is usually expressed in terms of a number of atomic layers, where a layer is defined as a (001) plane that contains Zn and O atoms. The five outermost atomic layers of atoms are allowed to relax during the geometry optimizations, and the remaining atomic layers are kept fixed at the bulk geometry in order to hold the characteristics of a realistic surface.

3. RESULTS AND DISCUSSION

3.1 Structural Properties

To explore the structural properties of ZnO, the three geometrical structures namely Wurtzite, Zinc blende and Rocksalt with space groups P63mc, $F\bar{4}3m$ and Fm3m in the Hermann–Mauguin notation, respectively were simulated (Figure 1). The location of Zn/O atoms related to the mentioned structures is as follows; (1/3 2/3 0)/(1/3 2/3 0.382), (0 0 0)/(1/4 1/4 1/4), (0 0 0)/(1/2 1/2 1/2).

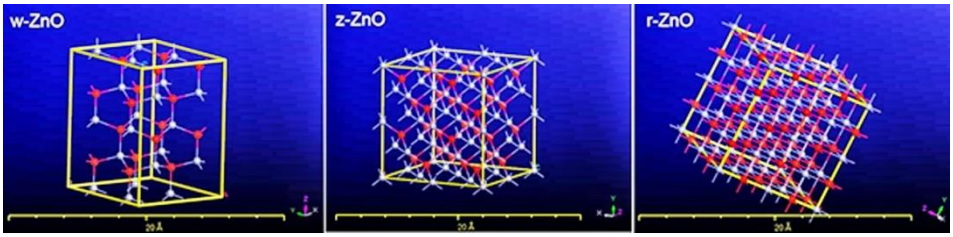

Fig. 1. Stick–and–ball representation of nanolayered ZnO crystal structures (2×2×2 supercells). Blue and red spheres denote Zn and O atoms, respectively.

To calculate the lattice parameters of ZnO in all three geometries, corresponding simulated unit cells were optimized. By calculating the total energy of optimized primitive unit cell at different volumes over a range of ±10% around equilibrium volume and fitting the data then with Murnaghan equation of state [16], obtained values of the equilibrium lattice parameters together with experimentally reported data and other theoretical results have been shown in Table 1.

TABLE 1. Lattice parameters of ZnO polymorphs along with bulk modulus B and its derivatives B'.

Structure	Method	Lattice parameters (Å)			B (GPa)	B'
		a	b	C		
Wurtzite	PBE (Present study)	3.250	3.250	5.204	150.3	4.4
	LDA (Wien2k) [5]	3.196	3.196	5.167		
	PBE (Wien2k) [5]	3.289	3.289	5.308		
	PBE96 (VASP) [6]	3.302	3.302	5.275		
	Experiment [17,18]	3.258, 3.249	3.258,3.249	5.220,5.206		
Zinc blende	PBE (Present study)	4.627	4.627	4.627	161.7	3.95
	LDA (Wien2k) [5]	4.501	4.501	4.501		
	PBE (Wien2k) [5]	4.626	4.626	4.626		
	PBE96 (VASP) [6]	4.634	4.634	4.634		
	Experiment [2]	4.470	4.470	4.470		
Rocksalt	PBE (Present study)	4.275	4.275	4.275	205	4.68
	LDA (Wien2k) [5]	4.223	4.223	4.223		
	PBE (Wien2k) [5]	4.339	4.339	4.339		
	PBE96 (VASP) [6]	4.340	4.340	4.340		
	Experiment [19]	4.271	4.271	4.271		

Total energy versus volume data for the Wurtzite structure of ZnO is shown in Fig.2. Meanwhile, the calculated bulk moduli (B) and the corresponding derivation (B') are given in Table 1.

Apparently, the lattice parameters are consistent with the listed theoretical calculations suggesting the credibility of our calculations.

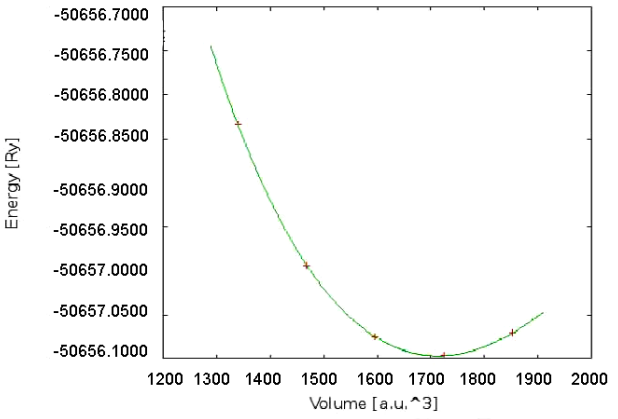

Fig.2. Total energy as function of primitive unit cell volume for ZnO in the phases of Wurtzite.

3.2 Electronic properties

To explore the electronic properties of ZnO, the electronic band structure that is pivotal in determining the electronic features, has been determined for three structural geometries. As it comes from the literature, the study of band structure of zinc oxide by theoretical approaches is still not up to the expectations. Within standard DFT, both LDA and GGA usually strongly underestimate the bandgap and overestimate the occupied cationic d bands. Owing to very simple form, they are not enough flexible to reproduce both the exchange–correlation energy and its derivative.

To realize more realistic electronic band structures, and to overcome the well known deficiency of DFT regarding energy gap underestimation with common XC functional, mBJ potential was employed in addition to PBE. The calculated band structures along the high symmetry directions in the Brillouin zone (BZ) of the zinc oxides are displayed in Figure 3.

The bandgap values computed according to GGA–PBE and GGA–mBJ are listed in Table 2, along with experimental values and other theoretical calculations.

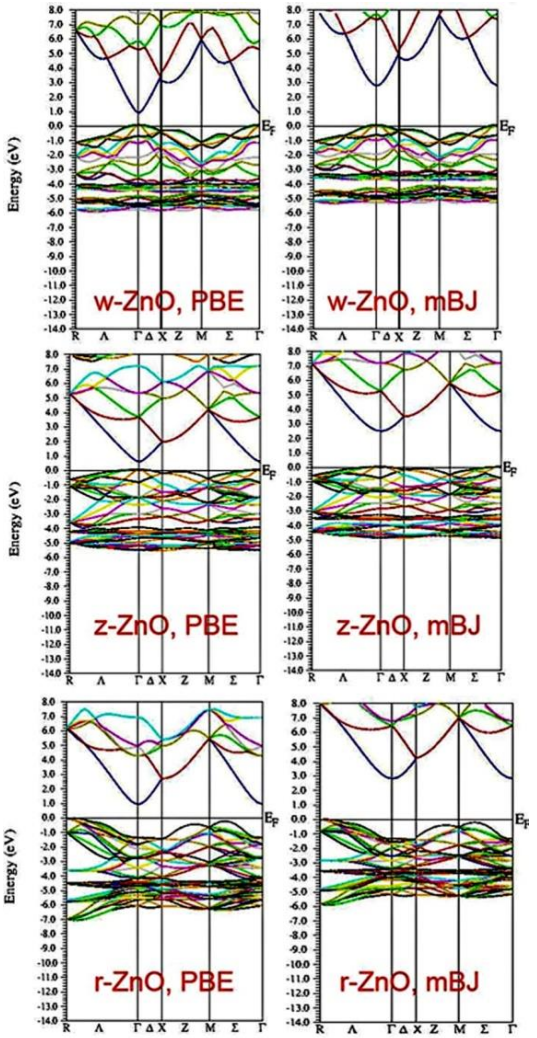

Fig.3. nanolayered ZnO band structures along the high–symmetry points in Brillouin zone.

The electronic structure of W–ZnO revealed direct energy gap nature since the valence band maximum (VBM) and conduction band minimum (CBM) are located at same Γ–point in the Brillouin zone. The corresponding energy gap calculated with PBE was of magnitude 0.98 eV which is believed to be underestimated due to the tendency of common GGA in over binding the electrons. The energy gap value has been improved to 3.01 eV by applying mBJ potential. The obtained band gap energy using mBJ fuctional seems more reliable and comparable with the experimental value 3.28 [20].

TABLE 2. Results of bandgap for ZnO polymorphs of Wurtzite, Zinc blende and Rocksalt. The results are compared with available experimental data and other first principle calculations.

Polymorph	Method	E_g (eV)
W-ZnO ($\Gamma\rightarrow\Gamma$)	GGA-PBE (Present study)	0.98
	GGA-mBJ (Present study)	3.01
	PAW-HSE06 [5]	2.19
	GGA-EV[22]	1.702
	LAPW- all electron GW[23]	2.44
	PAW-PW91 [24]	0.73
	Experiment [20]	3.28
Z-ZnO ($\Gamma\rightarrow\Gamma$)	GGA-PBE (Present study)	0.58
	GGA-mBJ (Present study)	2.59
	PAW-HSE06 [5]	2.22
	GGA-EV[22]	1.474
	PAW-PW91 [24]	0.64
	LDA [25]	0.71
	Experiment [21]	3.27
R-ZnO ($\Gamma\rightarrow L$)	GGA-PBE (Present study)	0.99
	GGA-mBJ (Present study)	2.81
	PAW-HSE06 [5]	2.93 (9 Gpa)
	GGA-EV[22]	1.683 (0 Gpa)
	PAW-PW91 [24]	1.97
	Experiment [26]	2.45±0.15 (0 Gpa)

The electronic structure of zinc blende depicted in Fig.2 exhibited the VBM and CBM at Γ–point in Brillouin zone, reflecting the direct energy gap in zinc blende geometry similar to wurtzite geometry. The computed energy gaps were of magnitude 0.58 eV and 2.59 eV with GGA–PBE and mBJ potential, respectively. The corresponding experimental value is 3.27 eV [21]. Comparing to other results in Table 2, mBJ result shows much better agreement with the experimental value. The difference of bandgap between W– and Z–ZnO is affected by the difference of the second neighbors [5]. Compared with the experimental data [20,21] of fundamental gap for B4 and B3 structures, our bandgaps are closer to the experiments but still underestimate by 8% and 20%, respectively. One main source of error can be linked to the fact that the Zn 3d level is too shallow. As it comes from the results, one can clearly see that the GGA–mBJ scheme is better than other theoretical calculations that some of them were given in Table 2.

In contrast to w– and z–ZnO the electronic structure of r–ZnO shows indirect energy gap. The VBM and CBM are positioned at L and Γ–points respectively. The calculated indirect bandgap with GGA–PBE and mBJ was 0.99 eV and 2.81 eV, respectively. The mBJ calculated value is larger than the experimental value of 2.45 eV [26]. This overestimation might come from too much of exact

exchange in GGA–mBJ. Another aspect of the evaluated band-structures is the existing degeneracy of almost all cases. For instance, the heavy-hole state in the wurtzite phase is doubly degenerated. In the layered ZnO, the heavy-hole state splits into two different bands at the Γ point, one is located at the top of the Γ point and the other shifts towards the low-energy level. For B4 phase there are two Zn and O atoms in the unit cell, thus its phonon dispersion consists of 12 branches whose group-theoretical analysis at the Brillouin-zone center (i.e. Γ point) yields a decomposition into $2A_{2u}+2B_{1g}+2E_{2g}+2E_{1u}$, where E_{2g} and E_{1u} are double degenerate modes.

One crucial factor in the expressions for electrical and optical properties of materials is the effective mass of charge carriers.

The effective mass of electron (m_e^*) was calculated by fitting the conduction bands minima to the parabola according to the expression $E = \hbar^2 k^2 / m_e^* m_e$ where me stands for rest mass of electron. The expression for *m** in isotropic solids can be written as $1/m^* = 1/\hbar^2 k \, dE/dk$. Then, the effective mass can be calculated as $m^* = \hbar^2 / \partial^2 E / \partial k^2$. The evaluated effective masses were listed in Table 3 in comparison with the other theoretical and experimental reported values. As it comes from the results, a quite good consistency exists between the calculated values here and the reported data of the other researchers.

TABLE 3. Calculated effective mass components for the Wurzite (B4), Zincblende (B3), and Rocksalt (B1) structures compared with theoretical results.

Structure	Reference	$m_e^*(\Gamma)$
W-ZnO	Present study (GGA-PBE)	0.311
	Present study (GGA-mBJ)	0.561
	[5]	0.517(0 Gpa)
	[27]	0.32
	[28]	0.30
	Experiment[29]	0.3
Z-ZnO	Present study (GGA-PBE)	0.209
	Present study (GGA-mBJ)	0.502
	[5]	0.242(0 Gpa)
	[30]	0.23 (0 Gpa)
R-ZnO	Present study (GGA-PBE)	0.308
	Present study (GGA-mBJ)	0.473
	[5]	0.255 (0 Gpa)
	[30]	0.22 (0 Gpa)

For a detailed overview of the electronic structure of W–, Z–and R–ZnO, the total DOS were determined with GGA–PBE and mBJ (Figure 4). The schematic representation of the total DOS calculated using GGA–mBJ shows that the VB

for ZnO is mostly dominated by Zn–d and O–p states. The two phases exhibit similar crystal symmetry and hybridization of states, with Zn atoms tetrahedral coordinated to O atoms. Both structural systems have strong hybridization of Zn–d and O–p states at the Γ point in the BZ, which causes coulomb repulsion and pushes the VB in the vicinity of Fermi level. Meanwhile, the calculated DOS diagrams suggest that the lower part of the valence band is dominated by the O–2s orbital and the upper part by the O–2p orbital. For zinc blende ZnO, it has been proved that the p–d repulsion is the source of the anomalous valence band structure [31].

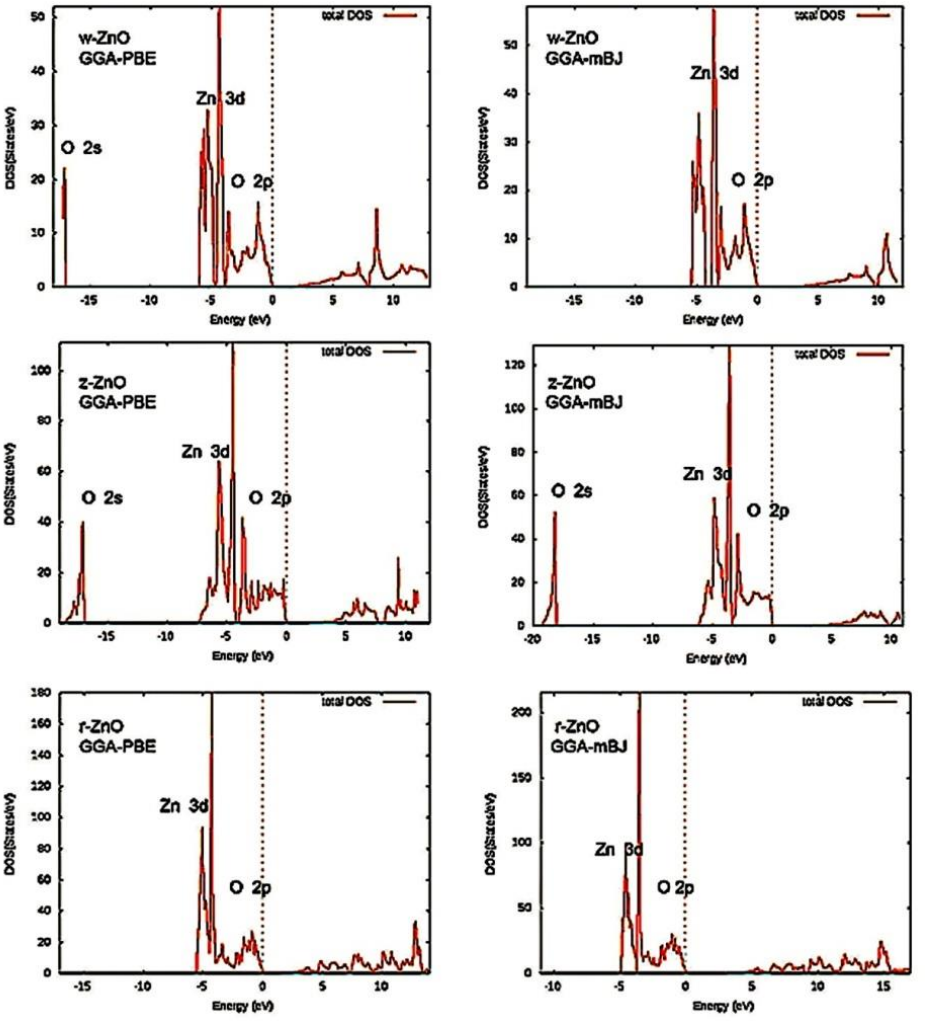

Fig. 4. Total density of states for w–, z– and r–ZnO phases according to GGA–PBE and GGA–mBJ exchange correlation potentials.

3.3 Optical Properties

In order to describe the optical properties of the materials, it is necessary to calculate the dielectric function $\varepsilon(\omega)=\varepsilon1(\omega)+i\varepsilon2(\omega)$, which is mainly contributed from the electronic structures. The ε1 and ε2 are the real and imaginary parts of dielectric function, respectively. The dielectric function describes the optical transitions that occur either among inter bands or intra bands. A schematic overview of the dispersive part ε1(ω) and the absorptive part ε2(ω) for the three ZnO phases calculated using GGA–PBE and GGA–mBJ are shown in Figure 5.

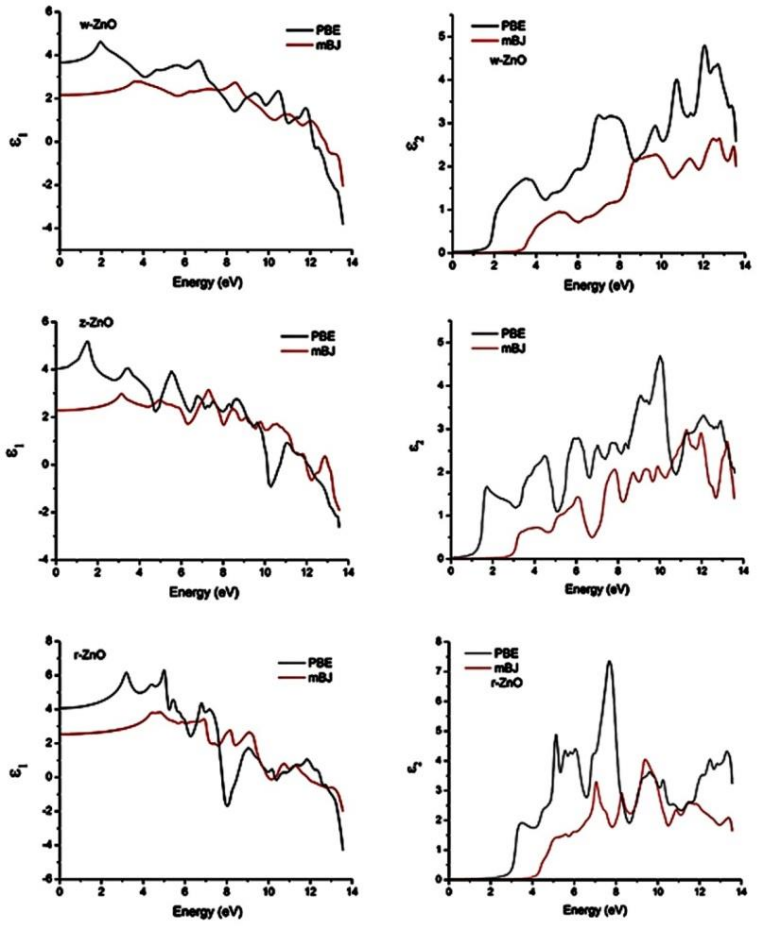

Fig.5. The real part ε1 and imaginary part ε2 of the dielectric function of nanolayered ZnO polymorphs.

The first structure in the imaginary part of dielectric function appears in energy range 2–6 eV that corresponds to the optical transition between the VBM and CBM. Direct optical transition of electrons between Zn–4s and O–2p occurs in this energy range. The threshold energies for the first structure are comparatively higher with mBJ potential than GGA–PBE, because of the wider energy gap calculated with mBJ. This trend is observed for all the structures in the dielectric function and the other investigated optical constants. The second major structure in imaginary part was located within the energy range of 6–9 eV. Combined with DOS in Fig.3, this peak can be linked to the electronic transition which took place between O–2p and Zn–3d states.

Figure 6 shows the absorption coefficient (α) of ZnO in three geometries. From the figure we can see that the major peak in the GGA–PBE absorption spectrum for Wurtzite structure is at 10.86 eV. However, in mBJ spectra it occurs at higher energy of and 11.45 eV. For Zinc blende/Rocksalt phase, these peaks are in 10.17/7.85 and 12.05/9.92 eV respectively. The optical absorption mainly originates from interband electron excitation between the valence and the conduction bands. All of the absorption peaks can be corresponded to the peaks of ε2 spectra for GGA–PBE and mBJ in Wurtzite, Zinc blende and Rocksalt phases deduced from the same electron transition. For instance, the first absorption peak corresponding to the first peak of ε2 spectra, deduced from the direct electron transitions from the O–2p states in valence band to the Zn–4s states in conduction band.

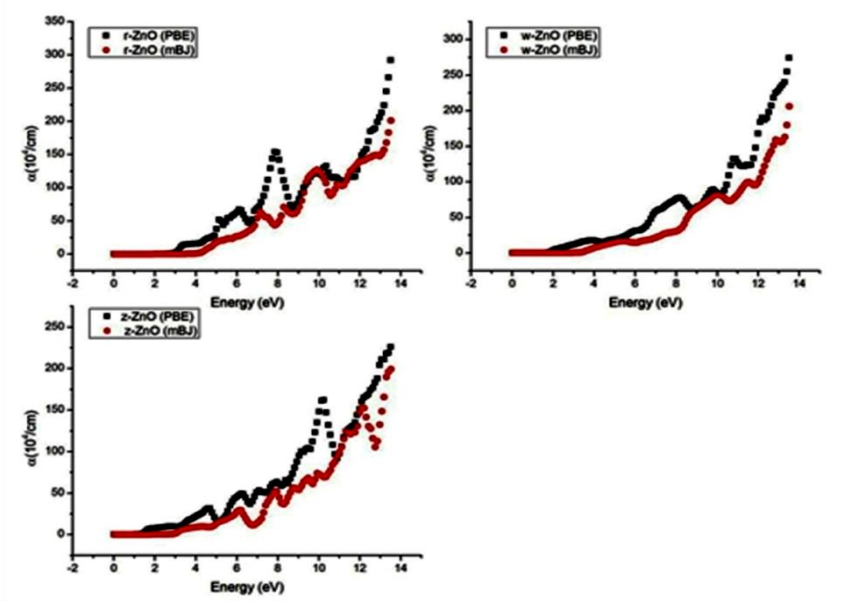

Fig.6. The calculated absorption coefficient for nanolayered ZnO structures of wurtzite, zinc blende and rocksalt.

Furthermore, from the absorption edge of absorption coefficient a qualitative perception of optical bandgap can be attained. From the extrapolating the edge of spectra for each sample and intercept with the horizontal axes (*hv*) the approximate value of bandgap can be evaluated. As it is seen visually, the trend of the graphs is completely consistent with the bandgap variation of studied samples.

Figure 7. depicts the reflectivity and transmittance spectra (R&T) in Uv–vis region that revealed lower reflectivity from ZnO when exposed to light photons. The light transmittance was deduced as follows [8]

$$T = (1-R)^2 e^{-\alpha d} \tag{1}$$

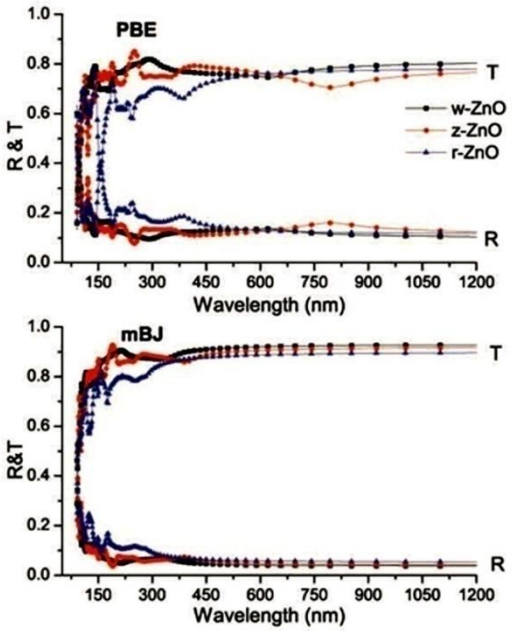

Fig.7. The calculated reflectivity and transmittance (R&T) for nanolayered ZnO structures of Wurtzite, Zinc blende and Rocksalt in Uv–vis region.

We calculated the light transmittance with the thickness (d) of 200 nm. As it comes from the figure, mBJ results show higher/lower transmittance/reflectance than that of PBE. The average transmittance values are around 80% and 90% for PBE and mBJ, respectively. These results indicate that, with a certain thickness of the material, quite lower reflectivity along with very high transparency is attainable in visible light region (400–800 nm) and infrared region (800–1200nm). This property makes ZnO as one the best candidates for photovoltaic

applications. The results are consistent well with the experimental reports [20, 32].

For accurate modeling and designing of optical materials for devices, knowledge of the dispersion of the refractive indices of the medium is necessary.

The calculated refractive index for ZnO polymorphs in Uv–vis region is shown in Fig. 8. From PBE/mBJ calculations, the average refractive index of different structures lies between 2.05/1.55 and 2.22/1.67. For W–ZnO, these results coincide well with the reported experimental values [32,33]. However, experimental reports on the refractive index of Z– and R–ZnO are very rare. Nevertheless, the evaluated values for refraction in this study is very close to the results obtained by GGA, LDA ad LDA+U for W– and Z–ZnO [34]. The extinction coefficient refers to the inelastic scattering of the electromagnetic waves in the semiconductor such as the Compton effect, photoelectric effect, pair production effect and so on [33]. Totally, the refractive index and the extinction coefficient of the films have an inverse relation with the transmittance spectrum.

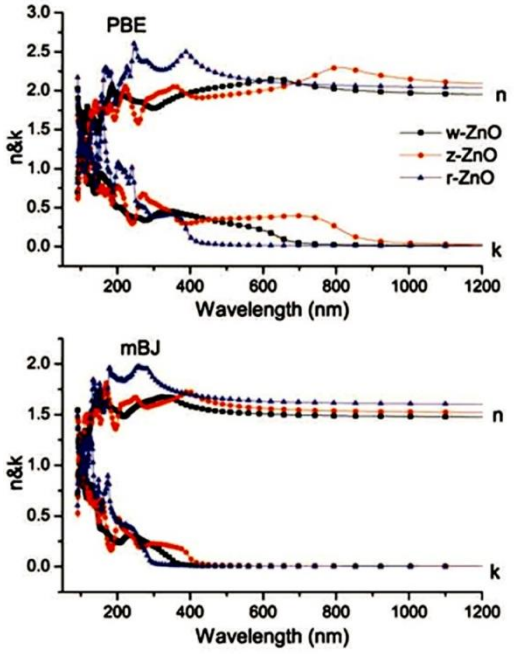

Fig.8. Refractive indices and extinction coefficient of nanolayered ZnO structures versus wavelength in Uv–vis region of spectrum calculated by PBE and mBJ exchange correlation potentials.

4. CONCLUSION

To survey the strengths and weaknesses of the popular PBE and mBJ exchange-correlation potentials, they were applied to study the electronic and optical properties of ZnO polymorphs in the 2×2×2 supercell model. The obtained lattice parameters at the level of GGA–PBE approach was found to be in good agreement with either previously reported theoretical or experimental work. It was found that the mBJ approximation gives more reliable bandgap values in comparison with PBE. Also, an obvious improvement was observed compared to the previous reports. The electron effective mass values at the bottom of conduction band were evaluated for the three studied geometries. In optical study, it was clearly observed that the spectra obtained by both approximations almost a similar trend; however, in the case of the optical constants, GGA–PBE approach seemed to give more reliable outputs than GGA–mBJ approach. As a conclusion, the DFT computational results for Wurtzite, Zinc blende and Rocksalt ZnO structures are very sensitive to the choice of the functional. Hence, an appropriate choice of XC functional in DFT calculations is very critical to obtain reliable results consistent with the experimental measurements.

ACKNOWLEDGMENT

The author is grateful to Islamic Azad University of Rasht for the financial support provided for this research.

REFERENCES

[1] A. Abdolahzadeh Ziabari, S.M. Rozati, *Carrier transport and bandgap shift in n-type degenerate ZnO thin films: The effect of band edge nonparabolicity*. Physica B 407 (2012) 4512–4517.
http://www.sciencedirect.com/science/article/pii/S0921452612008071

[2] Ü. Özgür, Y. I. Alivov, C. Liu, A. Teke, M. A. Reshchikov, S. Doğan, V. Avrutin, S. –J. Cho, H. Morkoç, *A comprehensive review of ZnO materials and devices.* J. Appl. Phys. 98 (2005) 041301.
http://adsabs.harvard.edu/abs/2005JAP....98d1301

[3] J. Wróbel, J. Piechota, *Structural properties of ZnO polymorphs.* Phys. Stat. Sol. (b) 244(5) (2007) 1538–1543.
http://onlinelibrary.wiley.com/doi/10.1002/pssb.200743399/full

[4] C. H. Bates, W. B. White, R. Roy, New *High-Pressure Polymorph of Zinc Oxide*. Science 137 (1962) 993.
http://adsabs.harvard.edu/abs/1962Sci...137..993B

[5] F. G. Kuang, X.Y. Kuang, Sh.Y. Kang, M.M. Zhong, A.J. Mao, *A first principle study of pressure-induced effects on phase transitions, band structures and elasticity of zinc oxide.* Mat. Sci. Semicon. Proc. 23 (2014) 63–71.
https://www.infona.pl/resource/bwmeta1.element.elsevier-d025c885-9ca3-3a80-9b8c-c3e2004b4a24

[6] M. P. Molepo, D.P. Joubert, *Computational study of the structural phases of ZnO.* Phys. Rev. B 84 (2011) 094110.
https://journals.aps.org/prb/pdf/10.1103/PhysRevB.84.094110

[7] M. Kalay, H.H. Kart, S. Özdemir Kart, T. Çağın, *Elastic properties and pressure induced transitions of ZnO polymorphs from first-principle calculations*. J. Alloys. Compd.484 (2009) 431–438.
http://www.sciencedirect.com/science/article/pii/S0925838809008548

[8] X. Si, Y. Liu, W. Lei, J. Xu,W. Du, J. Lin, T. Zhou, L.I. Zheng, *First-principles investigation on the optoelectronic performance of Mg doped and Mg–Al co-doped ZnO.* Materials and Design 93 (2016) 128–132.
http://www.sciencedirect.com/science/article/pii/S0264127515308923

[9] A. A. Peyghan, M. Noei, The alkali and alkaline earth metal doped ZnO nanotubes: DFT studies. B 432(2014) 105-110.
http://www.sciencedirect.com/science/article/pii/S0921452613006029

[10] H.I. Berrezoug, A.E. Merad, A. Zerga, Z.Sari Hassoun, *Simulation and Modeling of Structural Stability, Electronic Structure and Optical Properties of ZnO.* Energy Procedia 74 (2015) 1517–1524.
http://www.sciencedirect.com/science/article/pii/S1876610215014794

[11] J.P. Perdew, A. Ruzsinszky, G.I. Csonka, O.A. Vydrov, G.E. Scuseria, L.A. Constantin, X. Zhou, K. Burke, *Restoring the Density-Gradient Expansion for Exchange in Solids and Surfaces.* Phys. Rev. Lett. 100 (2008) 136406.
https://journals.aps.org/prl/abstract/10.1103/PhysRevLett.100.136406

[12] G.Y. Huang, C.Y. Wang, J.T. *Wang, Detailed check of the LDA + U and GGA + U corrected method for defect calculations in wurtzite ZnO.* Comput. Phys. Commun. 183 (2012) 1749–1752.
http://www.sciencedirect.com/science/article/pii/S0010465512001221?via%3Dihub

[13] A. D. Becke and E. R. Johnson, *A simple effective potential for exchange.* J. Chem. Phys. 124 (2006) 221101.
http://aip.scitation.org/doi/10.1063/1.2213970

[14] F. Tran, P. Blaha, *Accurate Band Gaps of Semiconductors and Insulators with a Semilocal Exchange-Correlation Potential.* Phys Rev Lett 102 (2009) 226401.
https://journals.aps.org/prl/abstract/10.1103/PhysRevLett.102.226401

[15] P. Blaha, K. Schwarz, G. Madsen, D. Kvasnicka, J. Luitz, An Augmented Plane Wave Plus Local Orbitals Program for Calculating Crystal Properties, Vienna University of Technology, Austria, 2014.
http://susi.theochem.tuwien.ac.at/reg_user/textbooks/usersguide.pdf

[16] A. Thilagam, D. Simpson, A. Gerson, *A first-principles study of the dielectric properties of TiO_2polymorphs.*J. Phys.: Condens. Matter 23 (2) (2011) 025901.
http://iopscience.iop.org/article/10.1088/0953-8984/23/2/025901/meta

[17] F.S. Decremp, F. Datchi, A.M. Saitta, A. Polian, S. Pascarelli, A. DiCicco, J.P. Itié, J,F. Baudelet, *Local structure of condensed zinc oxide*. Phys. Rev. B 68 (2003) 104101.
http://www-ext.impmc.upmc.fr/~decremps/SObject/Prb-5.pdf

[18] S. Desgreniers, *Structural and compressive parameters High-density phases of ZnO.* Phys. Rev. B 58 (1998) 14102–14105.
https://journals.aps.org/prb/abstract/10.1103/PhysRevB.58.14102

[19] H. Karzel, W. Potzel, M. Köfferlein, W. Schiessl, M. Steiner, U. Hiller, G.M. Kalvius, D.W. Mitchell, T.P. Das, P. Blaha, K. Schwarz, M.P. Pasternak, *Lattice dynamics and hyperfine interactions in ZnO and ZnSe at high external pressures.* Phys. Rev. B 53 (1996) 11425–11438.
https://www.ncbi.nlm.nih.gov/pubmed/9982760

[20] A. Abdolahzadeh Ziabari, F.E. Ghodsi, *Synthesis and characterization of nanocrystalline CdZnO thin films prepared by sol-gel dip-coating process.* Thin Solid Films 520 (2011) 1228–1232.
http://www.sciencedirect.com/science/article/pii/S0040609011013526

[21] A.A. Ashrafi, A.Ueta, H. Kumano, I. Suemune, *Role of ZnS buffer layers in growth of zincblende ZnO on GaAs substrates by metalorganic molecular-beam epitaxy.* J. Cryst. Growth 221 (2000) 435–439.
http://www.sciencedirect.com/science/article/pii/S0022024800007326

[22] U.H. Bakhtiar, R.Ahmed, R. Khenata, M. Ahmed, R. Hussain, *A first-principles comparative study of exchange and correlation potentials for ZnO*. Mater. Sci. Semicon. Proc.16 (2013)1162–1169.
http://www.sciencedirect.com/science/article/pii/S1369800112002909

[23] M. Usuda, N. Hamada, *All-electron GW Application to wurtzite ZnO calculation based on the LAPW method.* Phys. Rev. B 66 (2002) 125101.
https://journals.aps.org/prb/abstract/10.1103/PhysRevB.66.125101

[24] A. Schleife, F. Fuchs, J. Furthmüller, F. Bechstedt, *First-principles studies of ground- and excited-state properties of MgO, ZnO, and CdO polymorphs.* Phys. Rev. B 73 (2006) 245212.
https://arxiv.org/abs/cond-mat/0604480

[25] Y.Z. Zhu, G.D. Chen, H. Ye, *Electronic structure and phase stability of MgO, ZnO, CdO, and related ternary alloys.* Phys. Rev. B 77 (2008) 245209.
https://journals.aps.org/prb/abstract/10.1103/PhysRevB.77.245209

[26] A. Segura, J.A. Sans, F.J. Manjon, A. Munoz, M.J. Herrera–Cabrera, *Theoretical Study on the Origins of the Gap Bowing in MgxZn1–xO Alloys*. Appl. Phys. Lett. 83 (2003) 278–280.
http://file.scirp.org/Html/3-2190016_21382.htm

[27] Y.N. Xu, W.Y. Ching, *Electronic, optical, and structural properties of some wurtzite crystals.* Phys. Rev. B 48 (1993) 4335–4351.
https://journals.aps.org/prb/abstract/10.1103/PhysRevB.48.4335

[28] C.-Y. Ren, S.-H. Chiou, C.-S. Hsue, *Ga-doping effects on electronic and structural properties of wurtzite ZnO.* Physica B 349 (2004) 136.
http://www.sciencedirect.com/science/article/pii/S0921452604002029

[29] M. Oshikiri, K. Tanehaka, T. Asano, G. Kido, *Far-infrared cyclotron resonance of wide-gap semiconductors using pulsed high magnetic fields.* Physica B 216 (1996) 351.
http://www.sciencedirect.com/science/article/pii/0921452695005153

[30] Z. Charifi, H. Baaziz, A.H. Reshak, Phys. *Ab-initio investigation of structural, electronic and optical properties for three phases of ZnO compound.* Status Solidi B 244 (2007) 3154–3167.
http://onlinelibrary.wiley.com/doi/10.1002/pssb.200642471

[31] J.E. Jaffe, R. Pandey, A.B. Kunz, *Electronic structure of the rocksalt-structure semiconductors ZnO and CdO.* Phys. Rev. B 43(17) (1991) 14030–14034.
https://journals.aps.org/prb/abstract/10.1103/PhysRevB.43.14030

[32] X. Si, Y. Liu,W. Lei, J. Xu,W. Du, J. Lin, T. Zhou, L. Zheng, *First-principles investigation on the optoelectronic performance of Mg doped and Mg–Al co-doped ZnO*. Mater. Des. 93 (2016) 128–132.
http://www.sciencedirect.com/science/article/pii/S0264127515308923

[33] E. Amoupour, A. Abdolahzadeh Ziabari, H. Andarva, F.E. Ghodsi, *Influence of air/N_2 treatment on the structural, morphological and optoelectronic traits of nanostructured ZnO:Mn thin films.* Superlattices Microstruct. 65 (2014) 332–343.
http://www.sciencedirect.com/science/article/pii/S0749603613004096

[34] S. Zh. Karazhanov, P. Ravindran, A. Kjekshus, H. Fjellvåg, B. G. Svensson, *Electronic structure and optical properties of ZnX (X=O, S, Se, Te).* Phys. Rev. B 75 (2007) 155104.
https://arxiv.org/abs/0705.2550